ters. This scatter should be correlated between the two shifted lines.

It is clear that, by combining our data with those obtained in La Palma at about the same time, we will be able to reach a more complete understanding of these phenomena.

What Can We Expect from the Comparison of Optical and VLBI Data?

The VLBI observations are at present being reduced and should be available within a few months. Comparison of the two data sets will then be attempted. If moving features in the optical spectrum appear to be correlated with changing blobs in the radio jet, the origin of the Hα emission will be determined; this would provide a new possibility for mapping of the ionized gas structures, since until now imaging in the optical range has not shown any extended features around SS 433. In addition, detailed kinematic mapping of the propagation of the SS 433 jet could be envisaged with the Space Telescope, if the data correlation proves positive.

Particular attention will be paid to the following points:

- Does the bending of the radio jets affect the velocities of the moving lines?
- Is there any relation between the production of blobs and the equivalent width of the zero velocity Hα line?
- How is the spectacular appearance and disappearance of emission lines manifested in the radio data?

There are other X-ray stars which are known or suspected to present similarities with SS 433 and with the grander but more distant phenomena seen in AGNs (e.g., Sco X-1, Cir X-1, Cyg X-3, Her X-1 . . .), but none of them has revealed in such an open manner its intense private life. If SS 433 decided to cooperate with us last summer, important new information about the nature of X-ray binaries and even about jets in AGNs may result. It's now up to SS 433!

References

Abell G.O. and Margon B., *Nature* **279,** 701 (1979).
Clark D.H. and Murdin, P., *Nature* **276,** 44 (1978).
Fabian, A.C. and Rees, M.J., *M.N.R.A.S* **187,** 13 P (1979).
Margon, B., in *An. Rev. of Astr. and Astroph.* **22,** 507 (1984).
Schilizzi, R.T., Romney, J.D. and Spencer, R.E., IAU Symp. **110,** 289 (1984).

T Tauri Stars Through the Looking-Glass

U. FINKENZELLER and G. BASRI, Astronomy Department, University of California, Berkeley

The Red Queen shook her head. "You may call it 'nonsense' if you like," she said, "but I've heard nonsense, compared with which that would be as sensible as a dictionary!"

Preface

The CASPEC on the 3.6 m telescope is a very powerful new instrument for high dispersion spectroscopy. We have used it (in conjunction with an IDS) to obtain almost all the optical information possible on a number of T Tauri stars, namely calibrated resolved full spectral coverage. The analysis of such a large amount of information will take quite some time; the purpose of this contribution is primarily to acquaint other users with some of both the joys and pitfalls of this instrument which we feel are worthwhile to publicize. We also describe a little of the science in our particular project.

Chapter I

"It seems very pretty," she said [. . .], "but it's rather hard to understand!" (You see, she didn't like to confess, even to herself, that she couldn't make it out at all.)

T Tauri stars are young stellar objects with emission line spectra and complex atmospheres. Found in the upper right of the Hertzsprung-Russel diagram, they have effective temperatures from 3,000 to 6,000 K, and are estimated to be between 10^5 and 10^7 years old. Numerous observations in all parts of the electromagnetic spectrum indicate differences in activity levels of up to three orders of magnitude, together with temporal variations ranging from the beginning of astronomical data taking down to a few minutes. Due to their generally complex nature and the difficulties in obtaining a fully useful set of observational material, relatively little attention has been paid so far to self-consistent physical modeling of these stars. We have made an observational effort to provide new material which will allow the use of "classical" diagnostic tools to obtain detailed structures for most of the stellar atmosphere.

Guided by the rule that physical processes are most easily analyzed in their least complex manifestation, we have chosen seven low to intermediately active T Tauri stars (rather than exotic objects) from the spectral catalogue of Appenzeller et al. (1983). For further references on the stars, see also the original list of Schwartz (1977). The target objects span from G2 to M0 in spectral type, and from 5.8 to 0.5 in $L_\odot$ (see table). We have three pairs consisting of objects which are almost identical in most parameters, except for activity level. Together with a carefully chosen set of standard stars we are in a position to perform a differential activity analysis from the main sequence into the pre-main sequence domain by extrapolating proven diagnostic methods to slightly "perturbed" objects.

Chapter II

"I should see [. . .] far better," said Alice to herself, "if I could get to the top of that hill."

The full astrophysical potential for modeling of PMS stellar activity can only be realized if based on resolved flux calibrated, and high S/N spectra obtained for many diagnostics at the same time. With most instruments, the simultaneous demands of extreme spectral resolution and accurate spectrophotometry mutually exclude each other since the slit size affects both quantities in opposite ways. Thus, we used two different spectrographs concurrently: The ESO echelle spectrograph with CCD (CASPEC) at the 3.6 m and the IDS at the 1.5 m telescope. With a slit size of 3″ × 3″ at the former and 8″ × 8″ at the latter instrument we achieved resolutions of about 12,000 and 500–1,000, respectively. (The IDS grating was used in both first and second order.) The spectrophotometric observations had to be done strictly concurrently, since T

T TAURI STARS COVERED FROM 3800 TO 8700 Å

Star	Assoc.	m_v	Sp	$L_\odot$	$W_\lambda(H_\alpha)$	$W_\lambda(H_\beta)$	W_λ(HeI5876)	W_λ(LiI6707)
Sz06	Cham. 1	11.2	K2	2.34	−31.9	−2.30	—	0.43
Sz19	Cham. 1	10.6	G2	5.85	−14.6	−0.13	−0.04	0.23:
Sz65	Lupus 1	12.2	K7-M0	—	−24.2	+0.90	−0.79	0.61
Sz68	Lupus 1	10.5	K2	2.80	− 4.9	+1.95	—	0.42
Sz77	Lupus 1	12.5	M0	0.50	−15.1	−0.91	−0.21	0.60
Sz82	Lupus 2	12.2	M0	0.83	− 4.6	−0.03	−0.19	0.57
Sz98	Lupus 3	12.4	K8	0.72	−17.8	+3.39	−0.16	0.51

Tauri stars are expected to show irregular temporal variations, on top of which a rotational modulation may be imposed.

Apart from avoiding the principal limitations mentioned above, this scheme of observing allowed a most efficient use of the 3.6 m telescope, since no time had to be spent on observing mostly faint flux standards. Even more important, this technique avoids a number of cumbersome calibration problems which would have to be solved if one were to rely fully on CASPEC data alone (see below).

We were guided by the desire to cover the most important lines of CaII and hydrogen along with photospheric lines of all strengths, which demanded contiguous spectral coverage from 3800 Å to 8700 Å. Four echelle frames were required to span this spectral range, with a gap from 6700 Å to 7700 Å. With the 31.6 g/mm grating and the standard cross disperser complete order overlapping resulted, even in the near IR (8 Å at 8700 Å, rising to 36 Å at 3900 Å). A final total of 602 echelle orders of T Tauri stars and 560 orders of spectroscopic standards, supplemented by accompanying IDS scans, were obtained in three nights.

Chapter III

She puzzled over it for some time, but at last a bright thought struck her.

The IDS data were reduced according to standard procedures. The only minor problem arose with Baldwin and Stone's (1984) white dwarf standards which had to be resampled in order to tighten the grid for the response curves at the chosen resolution.

The CASPEC data were initially processed with the packages available in MIDAS for echelle work. However, we soon realized certain limitations which have to be faced when one is doing work in the ultraviolet where the spacing of the orders is steadily decreasing. (And it is in the ultraviolet that more astrophysical interesting lines happen to be than anywhere else.) At this point the reference to the external calibration from the IDS greatly helped in avoiding those internal problems shortward of 5000 Å as described below.

In an echelle frame centered at 4300 Å and taken with the standard cross disperser 33 orders are present, ranging from 3700 Å to 4765 Å. Since the RCA chip used is 321 pixels by 516 pixels, each order is about 9 pixels wide perpendicular to the dispersion, interorder background included. Under these limitations, useful work can only be done with the smallest entrance slit available, i.e. 3″ × 3″. Much thought has gone into the MIDAS echelle software which cannot be explained in detail here. The positions of the orders on the chip are recovered by two finding algorithms: Any specific order is first located once in the column running vertically through the middle of the frame and then defined by a maximun-following algorithm in both directions from this position. Both algorithms use polynomial fits, the recommended default degrees are 1 for the former and 2 for the latter.

Experience has shown, however, that it is hard to accomplish a global good fit for all regions within a frame. Polynomial degrees too low will not take into account small spatial variations or the slight distortions introduced by the spectrograph camera. On the other hand, polynomial degrees too high will introduce the well known wiggling effects which make the software slit run across the signal like a drunken driver speeding on a highway. Both effects are worst at the extreme ends of *all* orders in general, and the *uppermost* and *lowermost* orders of a particular frame. In the finally reduced spectrograms this can lead to ugly wiggling at wavelengths where the orders usually overlap and a loss of calibration at the very beginning and end.

CCD raw data should be subjected to a division by a flat field in order to account for sensitivity variations of various kinds on the chip. With CASPEC this is accomplished by illuminating the entrance slit of the spectrograph with either a built-in incandescent lamp or a bright screen attached to the dome. Dome flats necessitate very long exposure times, which is troublesome when one has to change the spectrograph settings often in a night. A well-known deficiency when using the incandescent lamp is that its light path through the optics is slightly different from the one taken by the stellar light. In the most general case this results in a small positional offset of the stellar and the flat field orders on the chip. For a proper pixel-by-pixel division the flat field orders should be appreciably wider than the stellar signal in order to ensure complete overlap by the flat. Otherwise, the stellar signal pixels would be divided by low or underexposed flat field pixels and give rise to spurious noise spikes in the output. Therefore, it is advisable to use a slit as long as possible for the flat without crowding the orders and choose the flat field exposure for the order tracing algorithms, rather than the stellar signal. Use of the stellar signal to trace the orders can be problematic if there are deep absorption lines in the spectrum. The fact that there is subtle, but not negligible, mechanical flexure in the spectrograph when moving the telescope from a program object to a standard star does not help. All these factors may cause the software slit to miss some fraction of the stellar signal, resulting in subsequent calibration problems. Finally, when the slit height is too small, there can be digital sampling errors as the software slit slants across the frame, leading to a few percent ripple in the measured total counts. These problems largely disappear if one is able to use a sufficient slit height, which can be done longward of 5000 Å where the interorder spacing is adequate.

Another effect to which close attention should be paid at all time during data reduction is that of scattered light in the spectrograph. This error source is particularly bothersome in the UV where its contribution is highest, and due to order crowding the standard countermeasures provided in MIDAS have the tendancy to either over or underestimate the background level. This correction affects absorption line depths or emission line heights in a direct way. There is no unequivocal recipe on how to proceed best. For example, we found that the deep absorption cores of the Ca II resonance

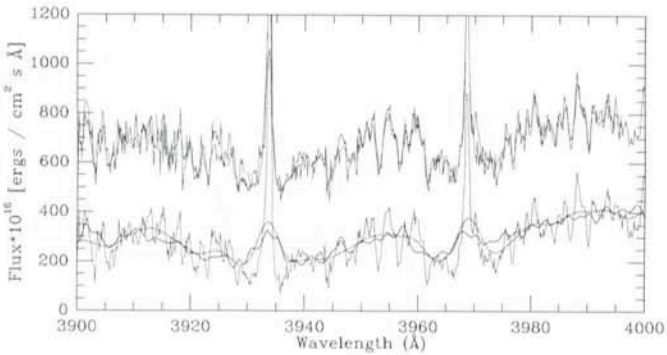

Fig. 1: *The flux calibration of the high resolution spectrograms was achieved by decreasing their resolution to the one of the (simultaneously obtained) photometric IDS spectra and a subsequent multiplication by the smoothed ratio of both signals. The figure shows (a) 5 individually calibrated orders, (b) the merged section of the echelle spectrogram (thin line), (c) this section after a convolution with a FWHM = 4.5 Å gaussian (dots), and (d) the original IDS spectrogram (fat line) of Sz06.*

lines had negative counts after treatment with MIDAS. This is due to an overestimation of the true background because of the order crowding. A more detailed study of individual frames is likely to be necessary in cases like this. Concerned readers may want to study the treatment of this problem elsewhere (c.f. the literature available on IUE high resolution data reduction).

In order to assign flux levels to the individual echelle orders we directly utilized the simultaneously obtained photometric IDS spectra. For calibration the resolution of the CASPEC spectrograms had to be decreased to that of the IDS. The values of 12,000 and 500/1 000 quoted above were obtained by evaluating the FWHM of the autocorrelation function of a comparison spectrogram. A convolution of the IDS data with gaussian functions of FWHM of 4.5 Å and 14 Å gave satisfactory results, although the instrumental profile of the IDS is not a strict gaussian. The flux correction is then the ratio of the smoothed echelle and unsmoothed IDS spectrogram. This generally well behaved function was approximated by a spline which disregarded high frequency noise in the IDS data. The echelle orders were then merged, using a full linear ramp length of 14 pixels at the edges and equal weights elsewhere. Fig. 1 gives an example of the procedure, showing (a) 5 individually calibrated orders, (b) the merged section of the echelle spectrogram, (c) this section after a convolution with a FWHM = 4.5 Å gaussian, and (d) the original IDS spectrogram. Note how well individual orders reproduce in the overlapping region. The final absolute accuracy of the photometric data is estimated by various cross checks with different flux standards to be on the order of 4–6 % over the whole range, and with relative errors within short wavelength intervals even smaller.

The RCA chip used for CASPEC shows fairly uniform quantum efficiency and only a very small fringing effect below 4 000 Å. Under these nearly ideal conditions one can work on frames using all the techniques mentioned above but without applying a flat field division. A quantitative comparison has shown that in the UV the final result was little affected by either using a flatfielded or a non-flatfielded frame.

Chapter IV

The White Queen whispered: "And I'll tell you a secret – I can read words of one letter! Isn't that grand? However, don't be discouraged. You'll come to it in time."

Due to the extremely high information content of the material obtained, our contribution at this time can be nothing more than an inadequate outline of a few empirical approaches we have taken so far. Because of the vast amount of work possible we are forced to initially emphasize certain approaches and targets. Thus, we are currently performing a case study with the stars Sz06 and Sz68, which are identical in most parameters (spectral type both K2, $L_\odot$ 2.3 vs. 2.8, v sini 34 vs. 42 km/s, W_λ (LiI6707) 0.43 vs. 0.42 Å), except for activity levels ($W_\lambda(H\alpha)$ –35.2 vs. –4.4 Å, and values of R_K whose ratio is 1.9). The star Sz19 of spectral type G2 is an ideal object to compare the detailed knowledge available for the sun to the T Tauri regime and is also receiving special attention. Far more interpretation is in progress and will be reported later. However, we would like to comment on a number of interesting results already available.

Values of v sini for the target stars can be obtained by either using Fourier, autocorrelation or direct matching techniques (c.f. Gray 1976). The available sampling step and S/N allows the detection of the characteristic zeros in the power spectra down to a lower limit of v sini = 14 km/s. Bouvier and Bertout (1985) have already given an outline of one method for applying these procedures to T Tauri stars. We were able to actually see the zeros directly by taking power spectra of various segments of the full merged echelle spectra and averaging these power spectra. The main advantage of the averaging is to greatly reduce what is referred to as "beating". (One should also bear in mind that the characteristic zeros are wavelength dependent, since v sini = $(.660 \times c) \div (\lambda \times \sigma_1)$, where σ_1 is the frequency of the first zero.) Very consistent results were obtained from the autocorrelation and direct matching determinations.

Our main interest centers on line ratios and absolute line and continuum fluxes. The approach to study the chromospheric structure is to consider the flux ratio of T Tauri stars relative to standard stars after the latter have been convolved with a proper rotational function (c.f. Strom 1983). Any chromospheric activity will then show up as excessive emission, related to particular lines. Because our material is calibrated, we can determine both general brightening of the UV continuum after dereddening and the enhanced emission in particular lines. The material can also be compared directly with spatially resolved spectroscopy of solar plages (e.g. LaBonte 1985).

Of course, both object and standard have to be moved to the same reference wavelength system; namely that of the stellar photosphere. Unfortunately, the resulting wavelength shift also affects the ever-present telluric lines, which already are in the same frame (and there are far more water lines at R = 12,000 than we ever dreamt of). Ideally, those lines should be removed *ab initio*, but this is rather hard to accomplish. As a result, virtual features can appear in the ratio plots. We have considered whether to present differences or ratios. The difference plots are only meaningful when made between spectra with continua normalized to the same value. Spectra in this form were made for the red frames. In the UV it is increasingly difficult to determine the true continuum, so we present ratios. Comparison between ratio and difference representations of the red data show no qualitative differences.

The first striking point to be seen in looking at the ratio plots (Fig. 2) is the high degree to which the weak and medium strength photospheric lines divide out. This gives us confidence that all the reduction stages have worked relatively well. Only the stronger absorption features in the standard star appear to fill up in the T Tauri stars. This phenomenon is easily seen the UV and infrared lines of neutral and ionized calcium, the Balmer lines, the sodium doublet, and a number of iron

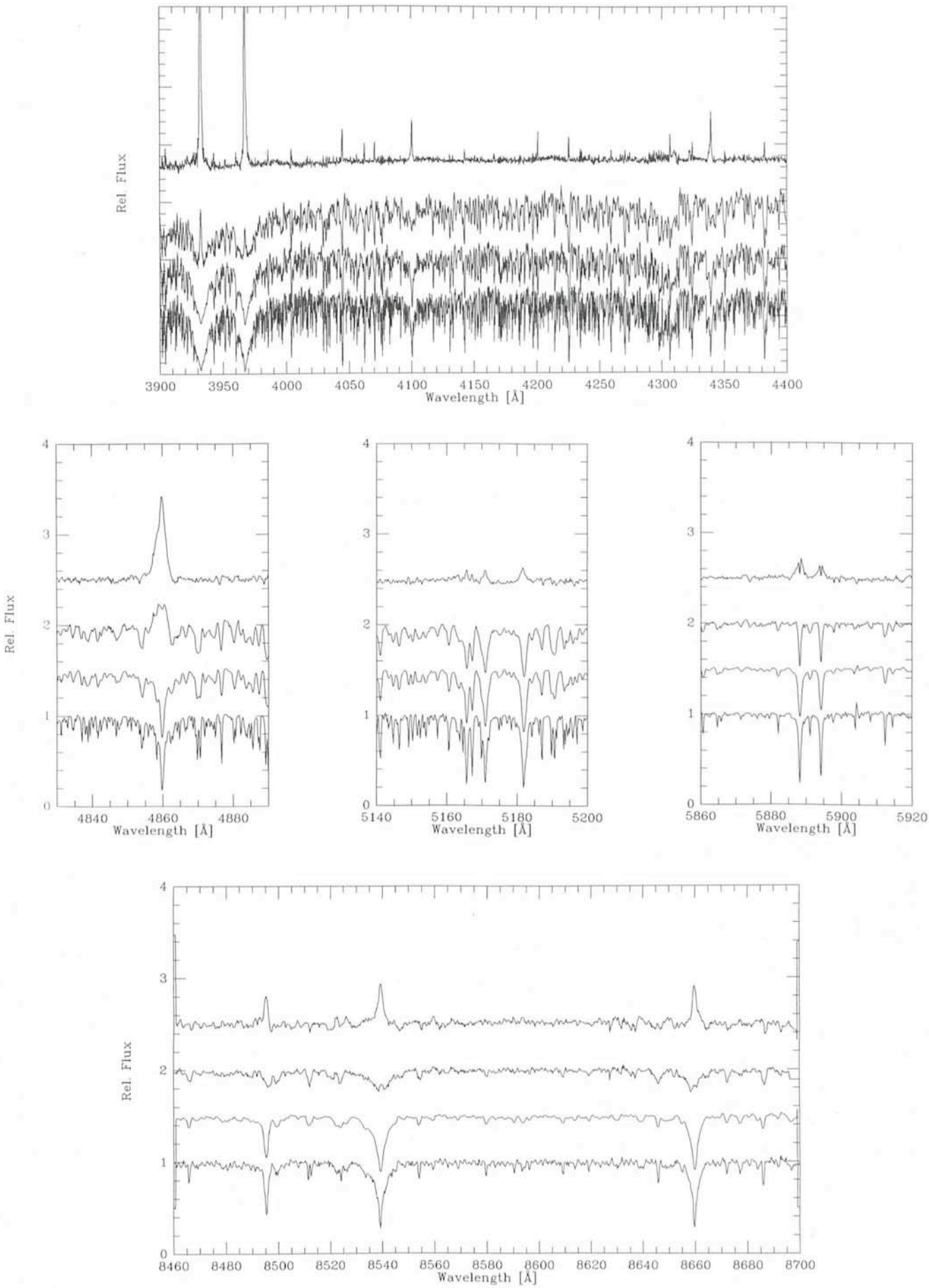

Fig. 2: *Illustration of excessive emission for Sz19 in the UV (a); at H_β, Mg I B, and N a D (b); and at the IR triplet (c). The figures give (from bottom to top) a spectroscopic standard (1); the standard convolved with a rotational function of v sini = 30 km/s (2); Sz19 (3); and the ratio (3):(2). Note that the two residual components of N a D obey a flux ratio of 2.0, and indicate the presence of an interstellar absorption feature, too.*

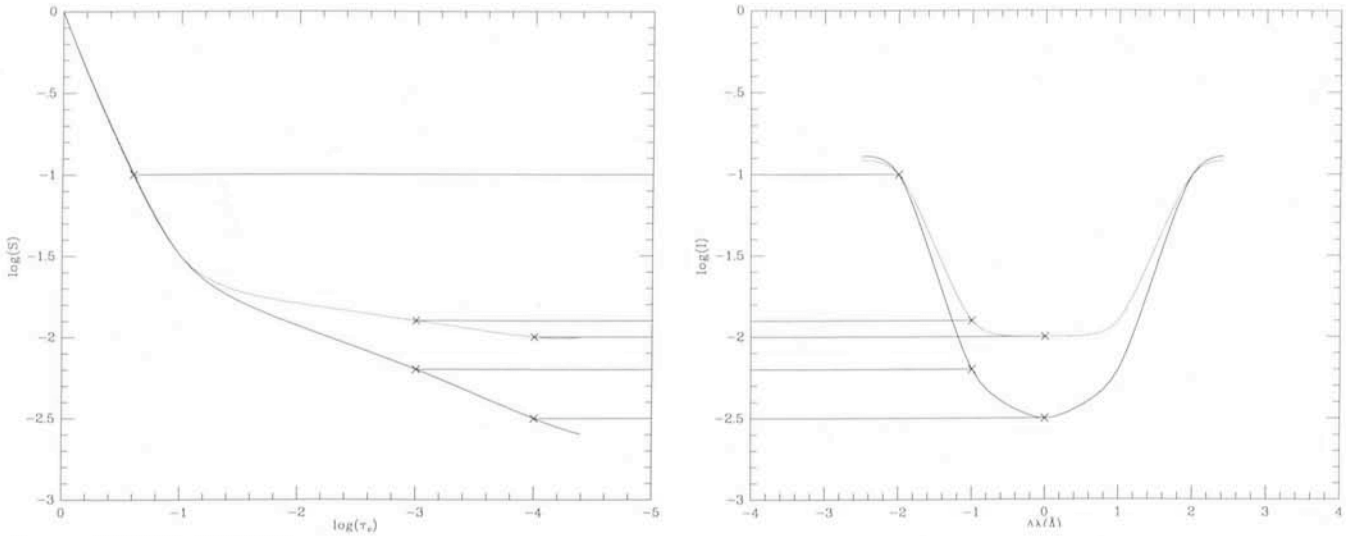

Fig. 3: *A schematic representation of the Eddington-Barbier relation in a spectral line and how an atmospheric perturbation can give rise to an emission feature in the ratio plots of Fig. 2. On the left are LTE source functions for a quiet (lower) and active (upper) star, with various line optical depth points marked. The way these translate to the line profile is shown on the right; the active star yields a brighter line core which appears as a positive ratio feature. The situation in a real star has a number of additional complications.*

lines. It is not caused by too low a zero level in the T Tauri UV spectra, since there are cases of lines with equal strength in the standard spectra of which only some appear as emission features in the ratio spectra (e.g. 4215 Å). The same effect is also seen in the red frames for which there is no question about the zero level. The stronger features are even apparent in the IDS spectra at much lower resolution. It is gratifying to note that the ratio spectra bear a close resemblance to solar chromospheric limb spectra. The lines which show up are those expected to be formed above the deep photosphere in the stellar atmosphere.

The qualitative explanation of this behaviour is straightforward: since the strong absorption lines probe a region further away from the stellar surface, this effect is presumably due to a differential increase of the source function at a given optical depth. Suppose one were to overlay a plot of the source function against optical depth (see Fig. 3) for a standard star and a T Tauri star (assuming that all lines share the same depth dependent source function, i.e. LTE). Then, for example, the residual intensity at the core of each line should reflect the value of this source function at approximately unit line center optical depth in each line. If we suppose the T Tauri star is identical to the standard star deep in the photosphere, and that its source function becomes increasingly larger as we move outward above a certain depth, then lines which become optically thick below that point will look the same in both stars, while lines formed above that point should have brighter cores in the T Tauri star. Thus, the depth of formation of lines which just begin to show up in the ratio plot is the depth at which the atmosphere of the T Tauri star is significantly perturbed relative to its main sequence counterpart. The fact that the weak lines are absent in the observed ratio spectra is proof that if you look deeply enough into a T Tauri star it looks "normal". By studying the excess emission as a function of depth, one obtains quantitative measures of the non-radiative heating structure of the atmosphere. Comparison of ratio plots for different stars gives an immediate useful characterization of the activity levels. Of course the real situation is not nearly as simple as outlined above; in the end one must take the presence of a feature in the ratio plot as a guide that detailed physical analysis of that line will be profitable. One must also keep in mind the possible circumstellar contributions especially in the very strong lines.

Ultimately, our purpose is to apply the full NLTE treatment of semi-empirical modeling to the data. We have, for example, calibrated line profiles for the Ca I, II resonance lines and Ca II IR triplet obtained at the same time. A model atmosphere which produces the desired synthetic profiles for these diagnostics can then be tested for consistency with the Balmer, Na D, Mg I B, etc. lines. Each line contributes a unique set of constraints to the emerging model. The model should also be able to explain the ratio spectrum and any UV continuum excess. We can hope to separate the near surface and circumstellar contributions to the spectrum and understand each with such detailed analysis. In the process, we will understand the relation of the pre-main sequence activity to its main sequence counterpart, and bring the level of ignorance about T Tauri stars to that for more studied examples of stellar activity.

References

Appenzeller, I., Jankovics, I., Krautter, J. 1983, *Astron. Astrophys. Suppl.* **53,** 291.

Baldwin, J. A., Stone, R.P.S. 1984, *M.N.R.A.S.* **206,** 241.

Bouvier, J., Bertout, C. 1985, *The Messenger* **39,** 33.

Carroll, L. MDCCCLXXI, Through the Looking-Glass and What Alice Found There, Macmillan.

Gray, D.F. 1976, The Observation and Analysis of Stellar Photospheres, Wiley, Toronto.

LaBonte, B.J. 1985, *Astrophys. J.,* preprint.

Schwartz, R.D. 1977, *Astrophys. J. Suppl.* **35,** 161.

Strom, S.E. 1983, *Revista Mex. Astron. Astrof.* **7,** 201.

List of ESO Publications

The following publications are still available:

Conference on "The Role of Schmidt Telescopes in Astronomy", Hamburg 21–23 March 1972. Proceedings. Ed. U. Haug. 160 p. DM 16.–

ESO/SRC/CERN Conference on "Research Programmes for the New Large Telescopes", Geneva, 27–31 May 1974. Proceedings. Ed. A. Reiz. 398 p. ISBN 3-923524-02-1. DM 40.–